Journal Pre-proofs

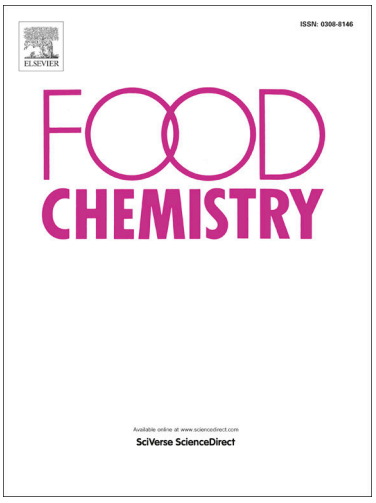

Thermal or membrane processing for Infant Milk Formula: Effects on proteins digestion and integrity of the intestinal barrier

Simona L. Bavaro, Gianfranco Mamone, Gianluca Picariello, Michael J. Callanan, Yihong Chen, André Brodkorb, Linda Giblin

PII: S0308-8146(21)00020-0
DOI: https://doi.org/10.1016/j.foodchem.2021.129019
Reference: FOCH 129019

To appear in: *Food Chemistry*

Received Date: 23 July 2020
Revised Date: 18 December 2020
Accepted Date: 3 January 2021

Please cite this article as: Bavaro, S.L., Mamone, G., Picariello, G., Callanan, M.J., Chen, Y., Brodkorb, A., Giblin, L., Thermal or membrane processing for Infant Milk Formula: Effects on proteins digestion and integrity of the intestinal barrier, *Food Chemistry* (2021), doi: https://doi.org/10.1016/j.foodchem.2021.129019

Thermal or membrane processing for Infant Milk Formula: Effects on proteins digestion and integrity of the intestinal barrier.

Simona L Bavaro[a], Gianfranco Mamone[b], Gianluca Picariello[b], Michael J Callanan[c], Yihong Chen[a,b], André Brodkorb[a] and Linda Giblin[a*]

[a] Teagasc Food Research Centre, Moorepark, Fermoy, Co. Cork, Ireland.

[b] Institute of Food Sciences, National Research Council, Avellino, Italy

[c] School of Biological Sciences, Cork Institute of Technology, Bishopstown, Cork, Ireland

***Corresponding author: Linda.giblin@teagasc.ie**

Declarations of interest: None

Abstract

Infant Milk Formula (IMF) is designed as a breastmilk substitute to satisfy the nutritional requirements during the first months of life. This study investigates the effects of two IMF processing technologies on cow milk protein digestion using an infant static *in vitro* gastrointestinal model. The degree of protein hydrolysis at the end of the gastric phase was 3.7-fold higher for IMF produced by high temperature (IMF-HT), compared to IMF produced by cascade membrane filtration (IMF-CMF), as assessed by free N-terminal groups analysis. The processing type also influenced the panel of bioavailable peptides detected in the basolateral compartment of Caco-2 monolayer exposed to gastrointestinal digested IMFs. In addition, IMF-CMF significantly increased tight junction protein, claudin 1, whilst IMF-HT significantly reduced tight junction integrity. In conclusion, producing IMF by CMF may preserve intestinal barrier integrity and can deliver its own unique inventory of bioavailable peptides with potential bioactivity.

1. Introduction

Infant formula is a valuable complete food for babies when the mother cannot, or does not want to breastfeed (Merewood et al., 2006). Conventionally, the majority of commercial infant formula products are formulated using cow's milk, as a substitute for human milk proteins combined with mixed vegetable oil as a substitute for human milk lipids. To ensure microbiological safety over shelf life, processing of infant milk formula (IMF) incorporates high temperature (HT) treatment. In addition, other heat treatments such as evaporation and spray drying are used to remove water from final product. These thermal processes result in unfolding of protein structure, cleavage and rearrangement of disulphide bonds, alternative aggregation of proteins and generation of Maillard reaction products (Chen et al., 2019). All of these process-induced modifications may change the structure of milk proteins in several ways, which can in turn affect the digestion and the overall physiological impact of these proteins (van Lieshout, Lambers, Bragt, & Hettinga, 2019).

This effect is especially relevant in early life, when bovine milk proteins are typically the sole source of food proteins and the digestive system is not yet fully developed. The intestinal immaturity is reflected in both enzymatic (type of enzymes and level of activity) and non-enzymatic (milk-based diet, frequency of feeding, bile salts concentrations, peristalsis) parameters compared to adult digestive conditions (Bourlieu et al., 2014; Mackie, Mulet-Cabero, & Torcello-Gómez, 2020). In this regard, Dupont et al. (2010) compared the effects of an *in vitro* infant model digestion and an adult model on the hydrolysis of milk proteins. β-casein was digested slowly, while β-lactoglobulin was degraded more extensively in the infant compared to the adult model due to the reduced amount of phosphatidylcholine in the infant model (Dupont et al., 2010). Ménard et al. (2018) observed that after 60 min of infant gastric digestion, 62% of intact proteins remained in the gastric phase, while in the adult model only 7% of intact proteins survived (Ménard et al., 2018). In turn, the peptides and amino acids

released during protein digestion can modulate the functions of intestinal barrier by influencing immune reactions, reducing oxidative stress, maintaining mucosal integrity and/or altering the expression and distribution of tight junction proteins (Arbizu, Chew, Mertens-Talcott, & Noratto, 2020; He et al., 2018; Zhang, Hu, Kovacs-Nolan, & Mine, 2015).

In the quest to produce humanized IMF, processing with reduced thermal loads while ensuring microbial safety, are under development. In this regard, we recently produced IMF by cascade membrane filtration (IMF-CMF) at pilot scale. We hypothesized that IMF-CMF will be different in terms of degree of protein hydrolysis and peptide release during gut transit compared to the IMF formulation produced by high temperature (HT). Recently several authors have investigated gastrointestinal digestion of different processing methods on dairy foods (Cilla et al., 2011; Mulet-Cabero, Mackie, Wilde, Fenelon, & Brodkorb, 2019; Rinaldi, Gauthier, Britten, & Turgeon, 2014). In particular, Rinaldi et al. (2014) observed sterilised milk resulted in faster digestion kinetic of casein in gastric phase than pasteurised milk (Rinaldi et al., 2014). Likewise, Cilla et al. (2011) showed that calcium and phosphorus bioaccessibility increased in milk based products produced by high-pressure processing versus conventional thermal treatments (Cilla et al., 2011).

The objectives of this study were to determine if processing by CMF would alter IMF peptide profiles released post gastrointestinal digestion. A further aim was to compare and contrast IMF-CMF to IMF-HT for promotion of intestinal barrier integrity, using 21 day old differentiated Caco-2 monolayer, as a model of the intestinal epithelium.

2. Material and Methods

2.1. Materials

Rabbit gastric extract was purchased from Lipolytech (France). Pancreatin (Sigma, P7545 , Ireland) was of porcine origin while bile (Sigma B8631, Ireland) was of bovine origin. Enzyme activities were determined as described in Brodkorb et al. (Brodkorb et al., 2019). Caco-2 cell line was purchased from the European Collection of Cell Cultures (collection reference: ECACC 86010202, UK). Ripa Buffer, Halt Protease and Phosphatase inhibitor (100×), and Pierce BCA Protein Assay Kit were purchased from Thermo Fisher Scientific (Ireland). Primary antibodies: rabbit monoclonal anti-zonula occludin 1 (ZO-1) (Cat. No. 339100), rabbit polyclonal anti-occludin (Cat. No. 71-1500), rabbit polyclonal anti- junctional adhesion molecule A (JAM-A) (Cat. No. 36-1700), rabbit polyclonal anti-claudin 1 (Cat. No. 51-9000) and anti-claudin 4 were purchased from Invitrogen (Invitrogen, USA). Secondary antibody goat anti-rabbit IgG (HRP) (Cat. No. 65-6120) was purchased from Invitrogen (USA). Ammonium bicarbonate, trifluoroacetic acid (TFA) and HPLC-grade solvents were purchased from Carlo Erba (Italy). All other reagents were purchased from Sigma Aldrich (Ireland).

2.2. Samples

HT and CMF formulas for infants from birth to 6 months were produced at pilot scale in the Biofunctional Engineering Facility, Teagasc Food Research Centre. The formulas were composed of 1.3 g of proteins (ratio casein/whey protein w/w: 40/60), 3.5 g of lipids and 7 g of carbohydrates per 12 g powder. IMF-HT was subjected to reverse osmosis for 20 min at 80°C, and then cooled to 50°C before being subjected to a heat-treatment of 80°C × 30s followed by standard UHT heating of 125°C × 5s. For IMF-CMF, formulation was filtered using cascade membrane filtration units of 1.4 µm and 0.2 µm at 50°C. Only the microfiltration

retentate was heat-treated at 80°C × 30s and then at 125°C × 5s. Both IMF-CMF and IMF-HT were homogenized and spray dried at inlet and output temperatures of 185°C and 80°C, respectively.

2.3. *In vitro* infant digestion protocol

The infant static *in vitro* digestion method mimics the upper gastrointestinal conditions of full-term infants, as described by Ménard et al. (2018). Briefly, HT or CMF IMF powder (2.25 g powder, which contained approximately 0.24 g protein) was reconstituted in 5 mL Milli-Q water. The oral phase was omitted while the gastric phase was performed using pepsin and lipase from rabbit gastric extract, based on a pepsin activity of 268 U/mL. Simulated gastric fluid was composed of NaCl and KCl fixed at 94 and 13 mM, respectively, and adjusted to pH 5.3 with 1M HCl. Gastric digestion was performed for 60 min in a shaking incubator (Excella E24, New Brunswick Scientific, USA) at 37°C at 15 rpm. The pH was then increased to 7 with 1 M NaOH (G60). The intestinal phase was performed using pancreatin (based on trypsin activity = 16 U/mL), and bovine bile extract at a final concentration of 3.1 mM. The simulated intestinal fluid was composed of 164 mM NaCl, 10 mM KCl and 85 mM $NaHCO_3$, adjusted to pH 7. Calcium chloride (3 mM) was added separately before the beginning of the intestinal phase. The digestion was performed for 60 min in a shaking incubator (Excella E24, New Brunswick Scientific, USA) at 37°C at 15 rpm. To stop the intestinal phase, 10 µL of protease and lipase inhibitors (1:1 0.1 M Pefabloc: 10mM Orlistat prepared in 100% Ethanol) per 0.5 mL digesta was added. For time point G0, the gastric phase was started and immediately halted by increasing the pH to 7 with 1 M NaOH. A simulated gastro-intestinal digestion (SGID) control was composed of gastrointestinal fluids, gut enzymes, bile salts and electrolytes but without the added infant formula. In summary, IMF Samples were collected at time zero (G0),

post gastric phase (G60) and post intestinal phase (I60), snap-frozen using liquid nitrogen and stored at −80° C until further analysis.

2.4. Protein analyses.

SDS-PAGE of G0, G60 and I60 of HT and CMF digested samples was performed using 4–12% polyacrylamide NuPAGE Novex Bis-Tris 12-well precast gels (Invitrogen, Ireland). Initially, the protein content in digested samples was determined by using a Pierce™ BCA Protein Assay Kit (Pierce Biotechnology, USA). To visualize protein hydrolysis, test samples (10 µg protein) were diluted with NuPAGE® LDS sample buffer with DL-dithiothreitol and denatured for 10 min at 70°C. MOPS buffer (1×) was employed as running buffer and electrophoretic separation was performed at 100 V. Gels were stained with Coomassie blue stain according to the manufacturer's protocol (InstantBlue, Expedeon, USA) and rinsed in distilled H_2O. Image analyses of gels were performed using Epson office in transmission mode (GE Healthcare, France).

2.5. Quantification of protein hydrolysis

Trichloroacetic acid (TCA) (3.12% final concentration) was added to the digested samples which resulted in the precipitation of insoluble proteins. The samples were centrifuged at 10,000 g for 30 min at room temperature and the supernatant was filtered using a syringe filter of PVDF 0.22 µm membrane (Millex-GV, Millipore, Ireland). The levels of free NH_2 groups were determined using the standardised o-phthaldialdehyde (OPA) spectrophotometric assay in micro-titre plates. OPA reagent consisted of 3.81 g sodium tetraborate dissolved in 80 mL Milli-Q H_20, dithiothreitol (0.088 g) and SDS (0.1 g). OPA (0.080 g) dissolved in 2 to 4 mL ethanol was then added and the final volume brought up to 100 mL with Milli-Q H_20. Different concentrations of standard L-leucine solution (prepared in phosphate buffered saline, PBS)

ranging from 0 to 10 mM were used to generate a calibration curve. Standard /sample (10 µL) was placed into each well and mixed with 200 µL of OPA reagent. The reaction was allowed to proceed for 15 min. The absorbance was measured at 340 nm using a multi-mode microplate reader (Synergy HT, BioTek Instruments, Inc., USA). Each measurement was performed in duplicate.

2.6. Cell Culture

Human intestinal epithelial cell line (Caco-2) was obtained from the European Collection of Cell Cultures (collection reference: ECACC 86010202, UK). Cells were grown in 75 cm^2 tissue culture flasks with the correspondent culture medium and kept at 37°C in humidified atmosphere containing 5% CO_2. Caco-2 cells were routinely cultured in Dulbecco's Modified Eagle Medium (DMEM) (glucose content of 4.5 g/L) supplemented with 10% (v/v) fetal bovine serum (FBS, Life Technologies, USA), 100 IU mL penicillin, and 100 µg/mL streptomycin (Thermo Fisher Scientific, USA). They were passaged by trypsinization with 0.05% trypsin-EDTA and resuspended in media every 3−4 days, upon reaching 80−90% confluence. Experiments were performed with cells at passage numbers 22−40.

2.7. Assessment of cell proliferation

Caco-2 cells were cultured in 96 well plates at a density of 5.0×10^4 cells mL with 100 µL complete DMEM at 37°C for 24 h. For cellular assays, triplicate samples from digestion experiments were pooled. I60 digested HT and CMF samples were diluted in Hank's Balanced Salt Solution (HBSS) and filtered through a 0.22 µm membrane; 10 µL of these solutions were added to the cells to give a total incubation volume of 100 µL with HBSS and a final sample protein concentration of 0 to 200 µg. For the buffer control, 10 µL of PBS was added to 90 µL HBSS. For gastrointestinal control, 10 µL gastrointestinal fluid containing gut enzymes, bile

salts and electrolytes was added to 90 µL HBSS. After 4 h, the supernatants were removed and 50 µL MTT solution (0.5 mg/mL) in HBSS medium were added. After a further 2h incubation, MTT solution was removed, 50 µL of 1:1 DMSO:ethanol was added and absorbance read at 570 nm in a Synergy HT microplate reader (BioTek Instruments, Inc., USA). Cell viability was referred to the HBSS control and expressed as percentage.

2.8. Transepithelial transport studies

Caco-2 cells were seeded on polyester permeable-membrane inserts (12 mm diameter, 0.4 µm pore size, 1.12 cm^2 growth area; Costar, USA) in 12-well transwell plates at a density of 6.0×10^4 cells/insert. The apical and basolateral compartments received 0.5 and 1.5 mL of the culture medium, respectively. Cells were allowed to grow and differentiate to form a confluent monolayer for 21 days, and the culture medium was replaced every other day. Monolayer integrity was assessed by measuring the transepithelial electrical resistance (TEER) values using a Millicell ERS-2 electrical-resistance system (Millipore, USA), and only cell monolayers with TEER values exceeding 700 $\Omega.cm^2$ were used for the permeability studies. TEER values > 700 $\Omega.cm^2$, indicated that monolayers had reached confluence and were polarized.

On treatment days, TEER values were recorded, and then monolayers were gently washed 2 times with HBSS and incubated for 30 min in HBSS at 37 °C. After the acclimatisation period, test samples (200 µg protein) were dissolved in HBSS to a final volume of 0.5 mL and added to the apical compartment. HBSS (1.5 mL) was added to the basolateral side. Control wells were monolayers treated with HBSS (buffer control) or monolayers treated with gastrointestinal fluids, gut enzymes, bile salts and electrolytes (SGID control). The cells were incubated at 37 °C for 4 h. The TEER value was measured before (0 h) and after incubation

(4h) to monitor the integrity of the monolayer. Finally, apical and basolateral solutions were collected and stored at−20 °C for further analyses.

2.9. Amino acid determination

Amino acid analysis was performed on G0, G60, I60, apical and basolateral samples. TCA (24%) was prepared using 100 mL of dH_20. The test samples were mixed thoroughly using a vortex. To 750 µL sample, 750 µL of 24% TCA was added. This mixture was mixed and allowed to stand in an ice-cold bath for 10 min. Samples were centrifuged for 10 min at 4000 x g. Supernatants were quantified using a Jeol JLC-500/V amino acid analyser (Jeol Ltd., Garden city, Herts, UK) fitted with a Jeol Na^+ high-performance cation exchange column. Tryptophan analysis was outsourced to MS-Omics (Denmark). Samples were derivatized with methyl chloroformate and then analysed by gas chromatography coupled with a quadropole mass spectrometry detector.

2.10. Tight junction analysis

The effects of SGID samples on intestinal barrier tight junction were assayed by Western blot analysis. After 4 h incubation with test samples, cell monolayers were scraped from the membrane and placed into a sterile eppendorf tube with 0.25 mL of RIPA buffer (Pierce Ripa buffer, Thermo Scientific, USA) in the presence of 1x Halt Protease and Phosphatase inhibitor cocktail. This cell extract was then subjected to one freeze thaw cycle, followed by 2 rounds of sonication on ice for 2 minutes using an ultrasonic bath Clifton, SW3H type, Nickel-Electro Ltd. (Weston-super-Mare, UK). The samples were then centrifuged at 13,000 x g at 4°C. Supernatant was collected and protein concentration quantified with Pierce™ BCA Protein Assay Kit (Pierce Biotechnology, USA), using BSA as the standard. SDS-PAGE gel loading buffer was added to I60 (25 µg protein). Proteins were separated by SDS-PAGE using

denaturing conditions (as above) on 4-12% w/v polyacrylamide gels and transferred onto a PVDF membrane (0.45μm) by using XCell II Blot Module (Thermo Fisher Scientific, Ireland) followed by secondary (HRP-conjugated) antibody incubation using Western breeze kit (Invitrogen, Ireland).

The membrane was blocked with Western breeze for 2 h to reduce nonspecific binding. The membrane was then incubated overnight at 4 °C with the primary antibody for either occludin (1:5000), JAM-A (1:5000) claudin-1 (1:5000), claudin 4 (1:5000), ZO-1 (1:200), or the mouse monoclonal anti-β-actin antibody (housekeeping) (1: 5000) diluted in blocking solution. The membrane was washed 3 times for 10 min with wash buffer and then incubated with the appropriate (mouse or rabbit) secondary IgG antibody for 2 h. After 5 min exposure to the chemiluminescent substrate, the immunoreactive proteins were visualized by a luminescent image analyser (LAS-3000; Fujifilm, Ireland). Densitometry analysis was performed and normalized against β-actin.

2.11. HPLC-Orbitrap MS/MS

HPLC-MS/MS analyses were performed using an Ultimate 3,000 nano-flow ultra-high-performance liquid chromatography (Dionex/Thermo Scientific, USA) coupled to a Q-Exactive Orbitrap mass spectrometer (Thermo Scientific, USA). Peptides were reconstituted in 2% acetonitrile/0.1% formic acid, and nearly 2 μg were loaded through Acclaim PepMap 100 trapcolumns (75-μm i.d. × 2 cm; Thermo Scientific, USA) using a FAMOS autosampler (Thermo Scientific, USA). Peptides were separated using an EASY-Spray TM PepMap C18 column (25 cm × 75μm i. d.) with 2 μm particles and 100-Å pore size (Thermo Scientific, USA). For the chromatographic step, eluent A was 0.1% formic acid (v/v) in LC-MS grade water, and eluent B was 0.1% formic acid (v/v) in acetonitrile. Separation was performed at a constant flow rate of 300 nL/min with a 2–50% gradient of B over 120 min after 5 min of

isocratic elution at 2% B. MS1 precursor spectra was acquired in the positive ionization mode scanning the 1,800–200 m/z range with resolving power of 70,000 full width at half maximum (FWHM), an automatic gain control (AGC) target of 1×10^6 ions, and maximum ion injection time of 100 ms. The spectrometer operated in full scan MS1 and data-dependent acquisition mode, selecting up to the 10 most intense ions for MS/MS fragmentation and applying a 12 s dynamic exclusion. Fragmentation spectra were obtained at a resolving power of 17,500 FWHM. To detect small peptides (<6-7 amino acid residues) singly charged ions were included in the MS/MS selection, along with 2-5 multiply-charged ions, using an exclusion list to prevent the repeated fragmentation of singly charged interfering compounds (De Cicco et al., 2019). Peptide samples prepared in triplicates were analysed by LC-MS/MS in three technical replicates. Spectra were elaborated using the software Xcalibur version 3.1 b (Thermo Scientific, USA).

Database Search and Peptide Identification LC-MS/MS

Raw data were analysed with the Andromeda tool of the MaxQuant software package (version 1.6.2.10). The searches were taxonomically restricted to the *Bos taurus* protein database downloaded from UniprotKB database on July 2019. Subsequently, the searches were refined using a manually constructed protein database containing the 30 most abundant cow-milk gene products inferred from proteomic-based investigations (Picariello et al., 2016). The search conditions included unspecific cleavage, no static modification, methionine oxidation, pyroglutamic acid at N-terminus glutamine, and serine/threonine phosphorylation, as variable modifications. The mass tolerance value was 5 ppm for the precursor ion and 10 ppm for MS/MS fragments. Peptide Spectrum Matches (PSMs) were filtered using the target decoy database approach at 0.01 peptide-level false discovery rate (FDR), corresponding to a 99% confidence score, and validation based on the *q*-value ($< 1 \times 10^{-5}$). Peptides sequences

identified by LC-MS/MS analysis in basolateral samples were also searched in Milk bioactive peptide database (http://mbpdb.nws.oregonstate.edu/) (Nielsen, Beverly, Qu, & Dallas, 2017) to identify potential bioactive peptide sequences

2.12. Statistical analysis

Gastrointestinal digestions were performed in triplicate. Culture experiments were performed in duplicate on 3 different days and the results are expressed as means ± SD. Statistical analysis was performed using GraphPad Prism 7.03 (GraphPad Software, Inc., USA). Significant differences between means were determined by using one-way ANOVA followed by post-hoc Bonferroni multiple comparison tests; P-value < 0.05 indicated statistical significance.

3. Results

CMF and HT powders were based on the design of first stage IMF (European Comission, 2006). The ratio between fat/protein/lactose, was 7:1.29:3.49, respectively, while the whey to casein ratio was 60:40. The IMF composition was unchanged between CMF and HT, but the processing differed with respect to thermal load. In particular, IMF-CMF was filtered using cascade membrane filtration units of 1.4 μm and 0.2 μm at 50°C. Only the microfiltration retentate was heat-treated at 80°C × 30s and 125°C × 5s. IMF-HT was subjected to reverse osmosis for 20 min at 80°C, then cooled to 50°C before being subjected to 80°C × 30s and 125°C × 5s. Both IMF-CMF and IMF-HT were homogenized and spray dried. Each powder (2.25 g powder, which contained approximately 0.24 g protein) was reconstituted in 5 mL H_2O and subjected to a SGID, based on the full term infant gut, as described by Ménard et al. 2018 (Ménard et al., 2018) with a higher gastric pH, shorter transit times and lower enzyme activities compared to those of the equivalent adult SGID protocol. Although the initial reconstituted powder concentration was higher than consumption recommendations (12g powder/100 mL),

this was necessary to ensure instrumentation detection of amino acids and peptides in downstream assays. IMF samples were collected at various time points (G0. G60, I60)

3.1 SDS-PAGE and degree of hydrolysis of IMF samples post upper gastrointestinal digestion

To track the fate of proteins during infant digestion, SGID samples were initially examined via SDS-PAGE followed by densitometer scans (Supplementary Fig. 1A-B). For each sample, the protein content was determined by using a Pierce™ BCA Protein Assay (Supplementary Fig. 2). SDS-PAGE indicated no differences in protein profiles between IMF-CMF and IMF-HT digesta at the same time points. Bands assigned to β-lactoglobulin (β-lg; 18.3 kDa) and α-lactalbumin (α-la; 14.2 kDa) appeared weaker in IMF-HT G60 compared to IMF-HT G0 by visual observation. Accordingly, densitometric analysis of all bands within a lane, showed no significant difference ($P>0.05$) between HT G0 and HT G60. By the end of the intestinal phase no intact proteins were observed in either CMF or HT samples (Supplementary Fig. 1A lanes 7 and 4). In addition, densitometric analysis (Supplementary Fig. 1B), revealed significant reduction ($P<0.05$) of band intensity ($P<0.05$) in CMF and HT at the end of the intestinal phase (I60) compared with time zero (G0) and post gastric phase (G60).

The degree of hydrolysis was assessed through the amount of free N-terminal groups by the OPA method (Fig. 1). At the end of gastric phase, IMF-HT had a much higher degree of hydrolysis than IMF-CMF, since free N-terminal groups were 147 and 40 μmol/mg of protein, respectively. By the end of the intestinal phase, the degree of hydrolysis was similar for both IMF processing methods (481 ± 7.7 μmol/mg of protein in IMF-HT I60 *vs* 471 ± 36.5 μmol/mg of protein in IMF-CMF I60). Interestingly, no significant difference was observed between degree of hydrolysis at the end of gastric phase of IMF-CMF G60 and time zero. On the

contrary, a significant difference ($P<0.05$) was recorded between IMF-HT at G60 compared to G0.

Moreover, both IMF-HT and IMF-CMF I60 samples had a degree of hydrolysis of 800% compared to G0 (481 and 471 µmol/mg of protein *vs* 51 and 41 µmol/mg of protein respectively).

3.3. Free amino acids analysis

The release of free amino acids from IMF powders produced by different processing methods was investigated (Table 1). As shown in Table 1, at time point G0 the concentration of free amino acids in IMF-CMF was 24.92 µmol/g powder, whereas in IMF-HT this value was 21.81 µmol/g powder. As expected, the SGID process released free amino acids totalling 603.63 µmol/g powder from IMF-CMF and 511.75 µmol/g powder from IMF-HT. Prior to SGID, the most abundant free amino acid in both IMF-CMF and IMF-HT was glycine and this was still the case after the gastric phase. In contrast the most abundant free amino acids at I60 were lysine and leucine for both powders, albeit larger quantities for IMF-CMF (85.94 and 140.10 in IMF-CMF *vs* 82.06 and 90.14 in IMF-HT). IMF-CMF released 57.42 µmol arginine /g powder at the end of intestinal phase (I60) whereas IMF-HT had negligible levels of arginine at the same time point. In addition, there was a relatively high level of histidine (50.03 µmol/g powder) in IMF-CMF at the end of intestinal digestion compared to 5.43 µmol/g powder in IMF-HT at I60. In contrast, phenylalanine was released at significant levels in IMF-HT at I60. At I60, tryptophan but not proline was detectable in both powders.

3.4 Cytotoxicity and transepithelial transport of HT and CMF digested samples on Caco-2 monolayer.

To explore the effects of IMF samples of the intestinal barrier permeability, 21-day old differentiated gut epithelium (Caco-2) monolayers were employed. Caco-2 monolayers maintain many morphological and functional traits that characterise the mature enterocytes of the small intestine such as cell polarisation, microvillus structure, active membrane peptidases, carrier-mediated transport systems and functional tight junctions between adjacent cells. Initially MTT cytotoxicity assays were performed on Caco-2 cells at various protein concentrations (5.0, 10.0, 25.0, 50.0, 100.0, 200.0 μg protein/cm^2) of I60 test samples to determine the working concentration for cellular assays. Concentration range was selected based on total surface area of the small intestine and the approximate daily intake of protein from IMF. For I60 test samples, protease and lipase inhibitors were added, samples underwent one freeze-thaw cycle and were filtered (0.22 μm) prior to cell exposure but, no heat inactivation step could be employed, as it would confound results.

None of the 4 concentrations tested were cytotoxic to Caco-2 cells allowing the use of 200 μg protein/cm^2 for permeability studies (Supplementary Fig. 3) with differentiated Caco-2 monolayers. Caco-2 monolayer tight junction integrity was monitored by TEER before and after a 4 hour exposure to I60 samples. At the outset, monolayers with TEER values > 700 Ω.cm^2 were considered to have intact tight junctions (Srinivasan et al., 2015). As shown in Fig. 2, IMF-CMF I60 sample did not reduce Caco-2 monolayer TEER values, compared to the HBSS buffer and to SGID controls. In contrast, IMF-HT induced a significant reduction of TEER values ($P<0.05$).

3.5 Tight junction proteins

To further assess the preserved functionality of tight junctions, Western blot analysis was performed on monolayer cell lysates using antibodies to typical biomarkers, namely occludin, claudin 1 and 4, ZO-1 and JAM-1 (Fig. 3). Densitometer scans using β-actin as control indicated that protein concentration of claudin 1 was significantly increased ($P<0.05$) and occludin tended to increase ($P = 0.01$) in Caco-2 monolayers exposed for 4 hours to IMF-CMF I60. No significant differences in these biomarkers were noted for the equivalent IMF-HT I60 sample compared to controls. Claudin 4, ZO-1 and JAM-1 levels in Caco-2 monolayers were unchanged with processing method or SGID.

3.6 Amino acid analysis of apical and basolateral compartments

Apical and basolateral compartment of Caco-2 monolayers exposed for 4 hours to I60 test samples were analysed for free amino acid composition (Table 2) and peptides sequences (Fig 4). Both the apical and basolateral compartments from IMF-CMF I60 experiments had the highest concentrations of total free amino acids (519.7 and 220.9 nM). Amino acid compositions of apical samples from IMF-CMF I60 and IMF-HT I60 digesta were similar, both reporting alanine as the most abundant free amino acid (77 and 68 nM). A notable difference was observed in the basolateral samples of Caco-2 monolayers treated with IMF-CMF I60 compared to IMF-HT I60, ie proline was detected with IMF-CMF I60 but not with IMF-HT I60 (Table 2). Tryptophan was not detected in both apical and basolateral compartments from IMF-CMF I60 or IMF-HT I60.

3.7 Peptide analysis, bioavailability and potential bioactivity

Peptide sequences identified by HPLC-MS/MS in the apical and basolateral samples from Caco-2 monolayers treated with IMF-HT I60 and IMF-CMF I60 are listed in Supplementary

Tables 1A-D. The unique peptide sequences identified are represented using Venn diagrams in Fig.4. In the apical compartment of Caco-2 monolayers exposed to IMF-CMF I60, 493 peptides were identified in addition to a further 107 capable of crossing the intestinal barrier, reaching the basolateral compartment. An additional 24 unique peptides were identified at the basolateral side (Fig. 4B). In the apical compartment of Caco-2 monolayers exposed to IMF-HT I60, 502 peptides were identified plus a further 83 peptides common to the basolateral side. The basolateral compartment also contained 22 unique peptides (Fig.4A).

Comparing peptide sequences in apical samples, 112 peptides were identified unique to IMF-CMF I60, 97 peptides were unique to IMF-HT I60, while 488 peptides were common to both IMF-HT and IMF-CMF I60 (Fig.4C). Similarly, in the basolateral compartment of Caco-2 monolayers, 47 peptides were identified unique to IMF-CMF I60, 21 peptides unique to IMF-HT I60 and 84 were common to both test samples (Fig. 4D).

Supplementary Fig. 4 displays pie charts illustrating breakdown of peptides in terms of protein origin. Specifically, 102 β-lactoglobulin peptides were identified in the apical compartment of Caco-2 monolayers exposed to IMF-CMF I60 compared to 66 β-lactoglobulin peptides in apical Caco-2 compartments treated with IMF-HT I60 (Supplementary Fig 4A-B). There were a higher number of whey derived peptides in the apical Caco-2 compartments treated with IMF-CMF I60 than with IMF-HT I60 (239 *vs* 151). Likewise, in the basolateral compartment of Caco-2 monolayers exposed to IMF-CMF I60 there were 42 whey derived peptides, among which 34 originated from β-lactoglobulin (Supplementary Fig 4 C-D). In line with the apical compartment, the total number of whey proteins-derived peptides at the basolateral side was higher for IMF-CMF I60 than for IMF-HT I60 (42 *vs* 29). Similarly, the number of casein peptides identified in basolateral samples was higher when Caco-2 monolayers were exposed to IMF-CMF I60 than IMF-HT I60 (82 *vs* 68) (Supplementary Fig.4C-D).

The MBPDP software assisted analysis of the peptides collected at the basolateral side enabled the identification of potential bioactive peptides. Supplementary Table 2 lists the known bioactive peptides and their derivatives found in the basolateral samples from Caco-2 monolayers exposed to IMF-HT and/or IMF-CMF at I60.

4. Discussion

In our *in vitro* models, IMF processing influenced (a) bioaccessibility and bioavailability of peptides, (b) intestinal barrier tight junction integrity and (c) the degree of protein hydrolysis in the infant stomach.

Thermal loads during processing will modify dairy protein structure which in turn will influence digestive enzyme accessibility, ultimately resulting in different peptide profiles with potentially different bioactivities. For instance, CMF processing certainly favours the bioaccessibility of β-lactoglobulin, as 102 peptides from this protein were identified in the Caco-2 apical compartment. Wada & Lonnerdal 2015 observed that native β-lactoglobulin in IMF resists gastric digestion but by the intestinal phase releases a large selection of peptides, many of which have notable bioactivities (e.g. dipeptidyl dipeptidase-4 (DPP4)-inhibitory and hypocholesterolemic peptides) (Wada & Lönnerdal, 2015). Many of the β-lactoglobulin peptides identified in Caco-2 basolateral compartments of our study have predicted ACE-inhibitory and antimicrobial activities. Interestingly, all β-lactoglobulin derived peptides of known bioactivity present in HT samples were also present in CMF samples but the opposite was not true. Notably, peptide GLDIQ was identified only in the Caco-2 basolateral solutions of IMF-CMF I60. This peptide derives from GLDIQK f(9-14), which has proven hypocholesterolemic and antihypertensive activities (Nagaoka et al., 2001; Pihlanto-Leppälä, Koskinen, Phlola, Tupasela, & Korhonen, 2000). β-casein peptide f(209-216), with sequence QEPVLGPV was also identified in basolateral samples from both IMFs. This peptide is a

potential precursor of QEPVL that significantly promotes proliferation of lymphocytes isolated from Balb/c mice when administered at 300 μg/ml. It also regulated Th1/Th2 cytokines by increasing serum IL-4 and IL-10 and decreasing IFN-γ levels after three weeks of oral administration at a concentration of 200 mg/kg (Jiehui et al., 2014).

Tight junction integrity of the *in vitro* intestinal epithelia also responded to processing type. IMF-CMF I60 increased tight junction protein claudin-1 and had a tendency to increase occludin compared to both control and IMF-HT I60. Occludin and claudin-1 are part of family of transmembrane proteins, that form the core of cell to cell tight junctions, controlling ion selectivity and permeability of the paracellular uptake pathway (Hartsock & Nelson, 2008). In particular, occludin is a 65-kDa protein thought to play both a structural and functional directly involved in barrier integrity (Lee, 2015). Claudin-1 is a 23 kDa protein that is directly involved in the regulation of paracellular permeability of ion channels (Zhu et al., 2019). Previous studies have shown that milk proteins can modulate the integrity and permeability of the intestinal barrier. For instance, Arbizu et al (2020) observed that bovine glycomacropeptide (100μg/ml) significantly increased claudin 1, claudin 3 and occludin in 15 day old Caco-2 monolayers and significantly increased TEER values of Caoc2-HT29MTX monolayers in the presence of the barrier disrupter, TNF-α (10 ng/mL), after 24 hours compared to media alone (Arbizu et al., 2020). Similar to our study, Arbizu et al. (2020) also noted that an increase in tight junction proteins does not necessarily result in TEER value increases. Whey protein isolate (100μg/mL) significantly increased mRNA transcript levels of claudin 1 in Caco-2 monolayers and protected Caco-2-HT29MTX permeability in the presence of TNF-α but had no effect on TEER values (Arbizu et al., 2020). Zhao et al.(2019) observed that 100 μg/mL bovine lactoferrin significantly increased claudin-1, occludin and ZO-1 mRNA transcripts by 2.45, 1.65, 1.82 fold respectively in Caco-2 cells compared to control media, and 1.22, 1.04, 1.69 fold in intestinal epithelial crypt cells (HIECs) compared to control media. In addition,

Caco-2 monolayer TEER values were increased by 41% and apparent permeability coefficients of sodium fluorescein significantly decreased, with both 50 and 100 μg/mL lactoferrin (Zhao et al., 2019). However the physiological relevance of adding intact proteins to intestinal cells is questionable. Yasumatsu & Tanabe 2010 reported that α_{s2}-casein peptide NPWDQ f(107-111) increased TEER values in a dose dependant manner (Yasumatsu & Tanabe, 2010). In our study, this peptide was present in Caco-2 apical compartments treated with either IMF. IMF-HT I60 significantly reduced TEER values compared to controls. It cannot be excluded that compounds, other than peptides, formed during HT processing (ie advanced glycation end products) may also reduce TEER values. However in previous work, treatment of Caco-2 monolayers to synthesized (20 μM) advanced glycation end products did not reduce TEER values (Chen et al., 2019).

Processing type also influenced rate of IMF digestion in our static infant gut model. At the end of the gastric phase, the protein in CMF samples was less hydrolysed with intact α-lactalbumin and β-lactoglobulin clearly visible. However, both processes resulted in a similar degree of hydrolysis at the end of the intestinal phase. IMFs currently on the market differ from breast milk in that they are routinely subjected to several heating steps during manufacture, which can include combinations of high-temperature short-time heating, evaporation, ultra-high temperature treatment and in-container batch sterilisation (Jiang & Guo, 2014). In this regard, it was reported that UHT milk undergoes a more rapid protein hydrolysis than unheated milk and pasteurized (72 °C for 15 s) milk during gastric digestion (Wada & Lönnerdal, 2014). In addition, heat treatment of milk resulted in a fragmented and crumbled coagulum under gastric conditions, leading to a greater rate of gastric protein hydrolysis (Bourlieu et al., 2014; Huppertz & Chia, 2020; Mulet-Cabero et al., 2019). The partial resistance of heat-treated whey proteins to hydrolysis during *in vitro* infant digestion could be due to weaker acidic conditions which reduce pepsin activity, or to aggregation and unfolding of the whey proteins occurring

during the heat treatment process that reduces enzyme (i.e. pepsin) accessibility (Halabi, Croguennec, Bouhallab, Dupont, & Deglaire, 2020; O'Loughlin, Murray, Kelly, Fitzgerald, & Brodkorb, 2012; Romano, Giosafatto, Masi, & Mariniello, 2015). Bourlieu et al. (2015) observed gradual hydrolysis of caseins at 60 min of gastric infant digestion, compared to the adult stage where caseins are extensively hydrolysed within 5 mins (Bourlieu et al., 2015). Rerat et al. (2002) revealed that the loss of nutritional quality due to pasteurization of cow milk for skim milk powder preparation is mainly driven by the reduced bioavailability of lysine, and to a lesser extent by the decreased digestibility of other essential amino acids such as phenylalanine, cysteine, aspartic acid and glycine (Rérat, Calmes, Vaissade, & Finot, 2002). It is important to note that both powders were spray dried but the time of heat exposure in this additional thermal step is extremely short and the denaturing effect of dairy proteins is known to be relatively small (>5% for skim milk) (Lin, Kelly, O'Mahony, & Guinee, 2018).

The low levels of free amino acids at G60 for both IMF agrees with the low degree of hydrolysis observed at the end of the gastric phase. In contrast, gastrointestinal digestion of IMF-CMF released considerable levels of free amino acids, including lysine and histidine, compared to IMF-HT. In addition, high concentrations of arginine (77 nM) and leucine (18.9 nM), as well as proline (25.5 nM), were detected in the basolateral compartment of Caco-2 monolayers treated with IMF-CMF I60. Arginine and leucine were predominant in Caco-2-HT29 or Caco-2 basolateral compartments post treatment with SGID commercial whey protein isolate (Corrochano et al., 2019) or SGID fresh whey (Goulart et al., 2014). Goulart et al. (2014) observed that Caco-2 monolayers exhibited a preference for the transport of certain amino acids such as leucine (Goulart et al., 2014). Caco-2 metabolism, amino acid transporters affinities and endo-/exo-peptidase activities are likely to play roles in promoting permeability of specific amino acids (Goulart et al., 2014). It is interesting to note that proline is detected in the Caco-

2 apical fluids after 4 hours incubation with IMF I60 samples, whilst it was absent in SGID IMF I60 samples.

Brush border hydrolysis also helps explain the differences in peptides in apical versus basolateral. In our study, the average length of IMF peptides on the basolateral side was 3-4 amino acids compared to an average length of 10-11 amino acids-long in the apical. Lacorix et al. (2017) studied the permeability of five bioactive milk peptides (LKPTPEGDL, LPYPY, IPIQY, IPI and WR) using Caco-2 cell monolayers. Although a small percentage (0.05% for LPYPY to 0.47% for WR) of the peptides were permeable across the monolayer, all five peptides were further hydrolysed (Lacroix, Chen, Kitts, & Li-Chan, 2017).

5. Conclusion

IMF processing modifies the structure of milk proteins, thereby affecting digestion patterns, bioaccessibility and bioavailability of resulting peptides. Furthermore intestinal barrier integrity and permeability of individual peptides across this barrier were altered by processing method. Whether or not this modulation is subtle or whether CMF provides an added health benefit requires further investigation. Certainly the modest heat treatment of IMF-CMF more closely resembles breast milk. Future work should include the development of an *in vitro* model of the infant gut barrier to investigate IMF-CMF ability to promote tight junction maturity. When or if permissible levels of advanced glycation endproducts in IMF are reduced, CMF is likely to be the easiest and economically feasible alternative to HT manufacture of IMF.

Acknowledgements: This work was funded by the Irish Department of Agriculture, Food and Marine Grant Number 15/F/604-TOMI. AB and LG are funded by Science Foundation Ireland (SFI) and the Department of Agriculture, Food and Marine on behalf of the Government of

Ireland under Grant Number [16/RC/3835]. We thank Dr. John Tobin, Teagasc whose team supplied the IMF powders for this research study, and Moorepark Technical service that performed free amino acids analysis.

Conflict of Interest

The authors declare no conflict of interest.

References

Arbizu, S., Chew, B., Mertens-Talcott, S. U., & Noratto, G. (2020). Commercial whey products promote intestinal barrier function with glycomacropeptide enhanced activity in downregulating bacterial endotoxin lipopolysaccharides (LPS)-induced inflammation *in vitro*. *Food & Function*. https://doi.org/10.1039/d0fo00487a

Bourlieu, C., Ménard, O., Bouzerzour, K., Mandalari, G., Macierzanka, A., Mackie, A. R., & Dupont, D. (2014). Specificity of Infant Digestive Conditions: Some Clues for Developing Relevant *In Vitro* Models. *Critical Reviews in Food Science and Nutrition*, *54*(11), 1427–1457. https://doi.org/10.1080/10408398.2011.640757

Bourlieu, C., Ménard, O., De La Chevasnerie, A., Sams, L., Rousseau, F., Madec, M. N., … Dupont, D. (2015). The structure of infant formulas impacts their lipolysis, proteolysis and disintegration during *in vitro* gastric digestion. *Food Chemistry*. https://doi.org/10.1016/j.foodchem.2015.03.001

Brodkorb, A., Egger, L., Alminger, M., Alvito, P., Assunção, R., Ballance, S., … Recio, I. (2019). INFOGEST static *in vitro* simulation of gastrointestinal food digestion. *Nature Protocols*. https://doi.org/10.1038/s41596-018-0119-1

Chen, Z., Kondrashina, A., Greco, I., Gamon, L. F., Lund, M. N., Giblin, L., & Davies, M. J. (2019). Effects of Protein-Derived Amino Acid Modification Products Present in Infant Formula on Metabolic Function, Oxidative Stress, and Intestinal Permeability in Cell Models. *Journal of Agricultural and Food Chemistry*. https://doi.org/10.1021/acs.jafc.9b01324

Cilla, A., Lagarda, M. J., Alegría, A., de Ancos, B., Cano, M. P., Sánchez-Moreno, C., … Barberá, R. (2011). Effect of processing and food matrix on calcium and phosphorous bioavailability from milk-based fruit beverages in Caco-2 cells. *Food Research International*. https://doi.org/10.1016/j.foodres.2011.07.018

Corrochano, A. R., Ferraretto, A., Arranz, E., Stuknytė, M., Bottani, M., O'Connor, P. M., … Giblin, L. (2019). Bovine whey peptides transit the intestinal barrier to reduce oxidative stress in muscle cells. *Food Chemistry*. https://doi.org/10.1016/j.foodchem.2019.03.009

De Cicco, M., Mamone, G., Di Stasio, L., Ferranti, P., Addeo, F., & Picariello, G. (2019). Hidden "digestome": current analytical approaches provide incomplete peptide inventories of food digests. *Journal of Agricultural and Food Chemistry*. https://doi.org/10.1021/acs.jafc.9b02342

Dupont, D., Mandalari, G., Mollé, D., Jardin, J., Rolet-Répécaud, O., Duboz, G., … Mackie, A. R. (2010). Food processing increases casein resistance to simulated infant digestion. *Molecular Nutrition and Food Research*. https://doi.org/10.1002/mnfr.200900582

European Comission. (2006). Commission Directive 2006/141/EC of 22 December on infant formulae and follow-on formulae and amending Directive 1999/21/EC. *Official Journal of the European Union*.

Goulart, A. J., Bassan, J. C., Barbosa, O. A., Marques, D. P., Silveira, C. B., Santos, A. F., … Monti, R. (2014). Transport of amino acids from milk whey by Caco-2 cell monolayer after hydrolytic action of gastrointestinal enzymes. *Food Research International*. https://doi.org/10.1016/j.foodres.2014.01.037

Halabi, A., Croguennec, T., Bouhallab, S., Dupont, D., & Deglaire, A. (2020). Modification of protein structures by altering the whey protein profile and heat treatment affects: *In vitro* static digestion of model infant milk formulas. *Food and Function*. https://doi.org/10.1039/d0fo01362e

Hartsock, A., & Nelson, W. J. (2008). Adherens and tight junctions: Structure, function and connections to the actin cytoskeleton. *Biochimica et Biophysica Acta - Biomembranes*. https://doi.org/10.1016/j.bbamem.2007.07.012

He, F., Wu, C., Li, P., Li, N., Zhang, D., Zhu, Q., … Peng, Y. (2018). Functions and

Signaling Pathways of Amino Acids in Intestinal Inflammation. *BioMed Research International*. https://doi.org/10.1155/2018/9171905

Huppertz, T., & Chia, L. W. (2020). Milk protein coagulation under gastric conditions: A review. *International Dairy Journal*. https://doi.org/10.1016/j.idairyj.2020.104882

Jiang, Y. J., & Guo, M. (2014). Processing technology for infant formula. In *Human Milk Biochemistry and Infant Formula Manufacturing Technology*. https://doi.org/10.1533/9780857099150.2.211

Jiehui, Z., Liuliu, M., Haihong, X., Yang, G., Yingkai, J., Lun, Z., … Shaohui, Z. (2014). Immunomodulating effects of casein-derived peptides QEPVL and QEPV on lymphocytes *in vitro* and in vivo. *Food and Function*. https://doi.org/10.1039/c3fo60657k

Lacroix, I. M. E., Chen, X. M., Kitts, D. D., & Li-Chan, E. C. Y. (2017). Investigation into the bioavailability of milk protein-derived peptides with dipeptidyl-peptidase IV inhibitory activity using Caco-2 cell monolayers. *Food and Function*. https://doi.org/10.1039/c6fo01411a

Lee, S. H. (2015). Intestinal Permeability Regulation by Tight Junction: Implication on Inflammatory Bowel Diseases. *Intestinal Research*. https://doi.org/10.5217/ir.2015.13.1.11

Lin, Y., Kelly, A. L., O'Mahony, J. A., & Guinee, T. P. (2018). Effect of heat treatment, evaporation and spray drying during skim milk powder manufacture on the compositional and processing characteristics of reconstituted skim milk and concentrate. *International Dairy Journal*. https://doi.org/10.1016/j.idairyj.2017.10.007

Mackie, A., Mulet-Cabero, A.-I., & Torcello-Gómez, A. (2020). Simulating human digestion: developing our knowledge to create healthier and more sustainable foods. *Food & Function*. https://doi.org/10.1039/D0FO01981J

Ménard, O., Bourlieu, C., De Oliveira, S. C., Dellarosa, N., Laghi, L., Carrière, F., … Deglaire, A. (2018). A first step towards a consensus static *in vitro* model for simulating full-term infant digestion. *Food Chemistry*. https://doi.org/10.1016/j.foodchem.2017.07.145

Merewood, A., Chamberlain, L. B., Cook, J. T., Philipp, B. L., Malone, K., & Bauchner, H. (2006). The effect of peer counselors on breastfeeding rates in the neonatal intensive care unit: Results of a randomized controlled trial. *Archives of Pediatrics and Adolescent Medicine*. https://doi.org/10.1001/archpedi.160.7.681

Mulet-Cabero, A. I., Mackie, A. R., Wilde, P. J., Fenelon, M. A., & Brodkorb, A. (2019). Structural mechanism and kinetics of *in vitro* gastric digestion are affected by process-induced changes in bovine milk. *Food Hydrocolloids*. https://doi.org/10.1016/j.foodhyd.2018.03.035

Nagaoka, S., Futamura, Y., Miwa, K., Awano, T., Yamauchi, K., Kanamaru, Y., … Kuwata, T. (2001). Identification of novel hypocholesterolemic peptides derived from bovine milkβ-lactoglobulin. *Biochemical and Biophysical Research Communications*. https://doi.org/10.1006/bbrc.2001.4298

Nielsen, S. D., Beverly, R. L., Qu, Y., & Dallas, D. C. (2017). Milk bioactive peptide database: A comprehensive database of milk protein-derived bioactive peptides and novel visualization. *Food Chemistry*. https://doi.org/10.1016/j.foodchem.2017.04.056

O'Loughlin, I. B., Murray, B. A., Kelly, P. M., Fitzgerald, R. J., & Brodkorb, A. (2012). Enzymatic hydrolysis of heat-induced aggregates of whey protein isolate. *Journal of Agricultural and Food Chemistry*. https://doi.org/10.1021/jf205213n

Picariello, G., Addeo, F., Ferranti, P., Nocerino, R., Paparo, L., Passariello, A., … Canani, R. B. (2016). Antibody-independent identification of bovine milk-derived peptides in breast-milk. *Food and Function*. https://doi.org/10.1039/c6fo00731g

Pihlanto-Leppälä, A., Koskinen, P., Phlola, K., Tupasela, T., & Korhonen, H. (2000). Angiotensin I-converting enzyme inhibitory properties of whey protein digests: Concentration and characterization of active peptides. *Journal of Dairy Research*. https://doi.org/10.1017/S0022029999003982

Rérat, A., Calmes, R., Vaissade, P., & Finot, P. A. (2002). Nutritional and metabolic consequences of the early Maillard reaction of heat treated milk in the pig. Significance for man. *European Journal of Nutrition*. https://doi.org/10.1007/s003940200000

Rinaldi, L., Gauthier, S. F., Britten, M., & Turgeon, S. L. (2014). *In vitro* gastrointestinal digestion of liquid and semi-liquid dairy matrixes. *LWT - Food Science and Technology*. https://doi.org/10.1016/j.lwt.2014.01.026

Romano, A., Giosafatto, C. V. L., Masi, P., & Mariniello, L. (2015). Impact of dehulling on the physico-chemical properties and *in vitro* protein digestion of common beans (Phaseolus vulgaris L.). *Food and Function*. https://doi.org/10.1039/c5fo00021a

Srinivasan, B., Kolli, A. R., Esch, M. B., Abaci, H. E., Shuler, M. L., & Hickman, J. J. (2015). TEER Measurement Techniques for *In Vitro* Barrier Model Systems. *Journal of Laboratory Automation*. https://doi.org/10.1177/2211068214561025

van Lieshout, G. A. A., Lambers, T. T., Bragt, M. C. E., & Hettinga, K. A. (2019). How processing may affect milk protein digestion and overall physiological outcomes. *Critical Reviews in Food Science and Nutrition*. https://doi.org/10.1080/10408398.2019.1646703

Wada, Y., & Lönnerdal, B. (2014). Effects of different industrial heating processes of milk on site-specific protein modifications and their relationship to *in vitro* and in vivo digestibility. *Journal of Agricultural and Food Chemistry*. https://doi.org/10.1021/jf501617s

Wada, Y., & Lönnerdal, B. (2015). Bioactive peptides released by *in vitro* digestion of

standard and hydrolyzed infant formulas. *Peptides*. https://doi.org/10.1016/j.peptides.2015.09.005

Yasumatsu, H., & Tanabe, S. (2010). The casein peptide Asn-Pro-Trp-Asp-Gln enforces the intestinal tight junction partly by increasing occludin expression in Caco-2 cells. *British Journal of Nutrition*, *104*(7), 951–956. https://doi.org/10.1017/S0007114510001698

Zhang, H., Hu, C. A. A., Kovacs-Nolan, J., & Mine, Y. (2015). Bioactive dietary peptides and amino acids in inflammatory bowel disease. *Amino Acids*. https://doi.org/10.1007/s00726-014-1886-9

Zhao, X., Xu, X. X., Liu, Y., Xi, E. Z., An, J. J., Tabys, D., & Liu, N. (2019). The *in vitro* protective role of bovine lactoferrin on intestinal epithelial barrier. *Molecules*. https://doi.org/10.3390/molecules24010148

Zhu, L., Han, J., Li, L., Wang, Y., Li, Y., & Zhang, S. (2019). Claudin family participates in the pathogenesis of inflammatory bowel diseases and colitis-associated colorectal cancer. *Frontiers in Immunology*. https://doi.org/10.3389/fimmu.2019.01441

Figure 1

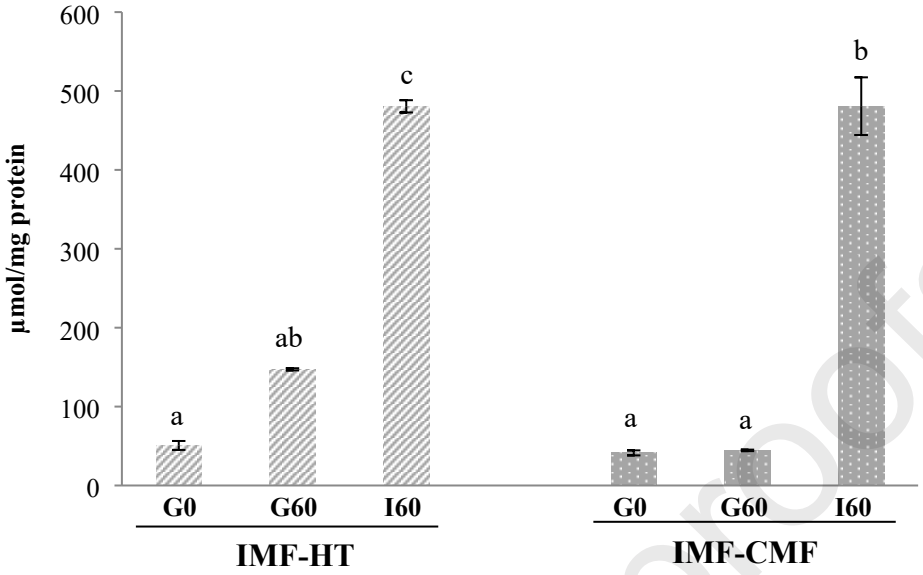

Fig 1. Concentration of free amine groups per mass of total protein in IMF-HT and IMF-CMF at initial gastric phase (G0), at the end of gastric phase (G60) and at the end of intestinal phase (I60). Each data point is the average of 3 independent replicates and error bars represent standard deviation. Statistical differences were assessed by one-way ANOVA and Bonferroni multiple-comparisons test. Different letters within a processing method indicate significant difference ($p<0.05$).

Figure 2

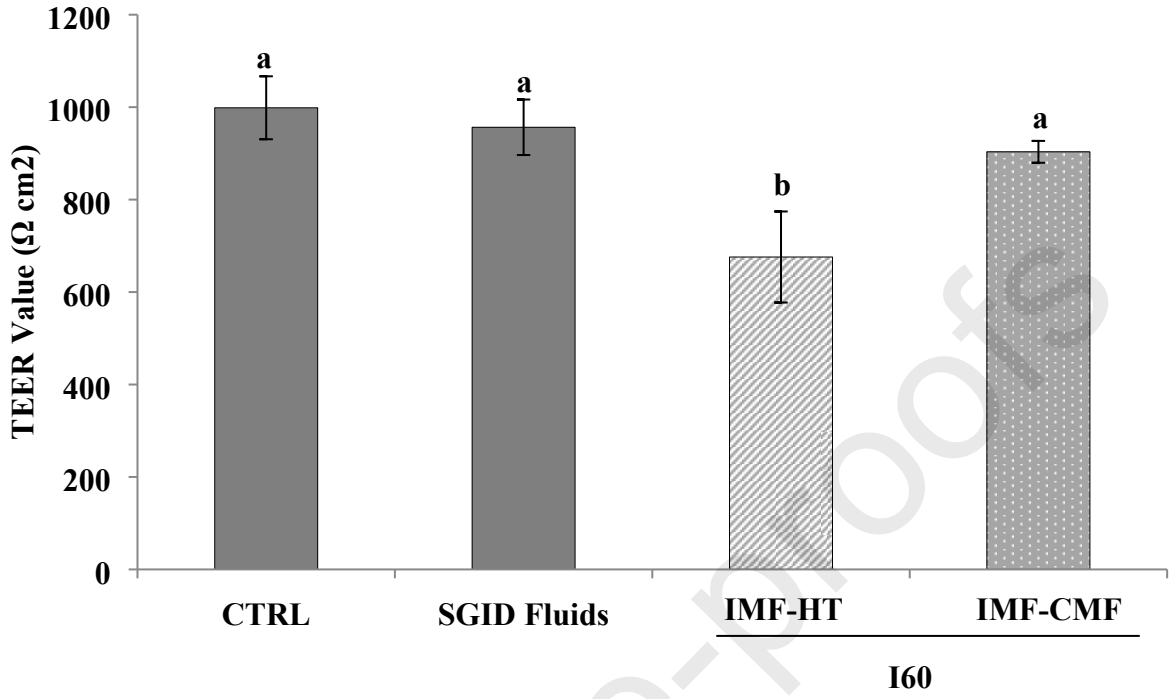

Fig 2. TEER values of Caco-2 monolayers treated with IMF-HT I60 and IMF-CMF I60 samples for 4 hours. The TEER values were recorded on day 21 differentiated Caco-2 cell monolayer exposed to test samples (200 µg protein/cm^2). Positive control (CRTL) was Caco2 monolayers treated with HBSS buffer only. SGID = Caco2 monolayers treated with SGID fluids plus enzymes. Experiment was repeated three times. Data are presented as means ± SD (n = 6). Statistical differences were assessed by one-way ANOVA and Bonferroni multiple-comparisons test, with different letters are significantly different ($p < 0.05$), from each other.

Figure 3

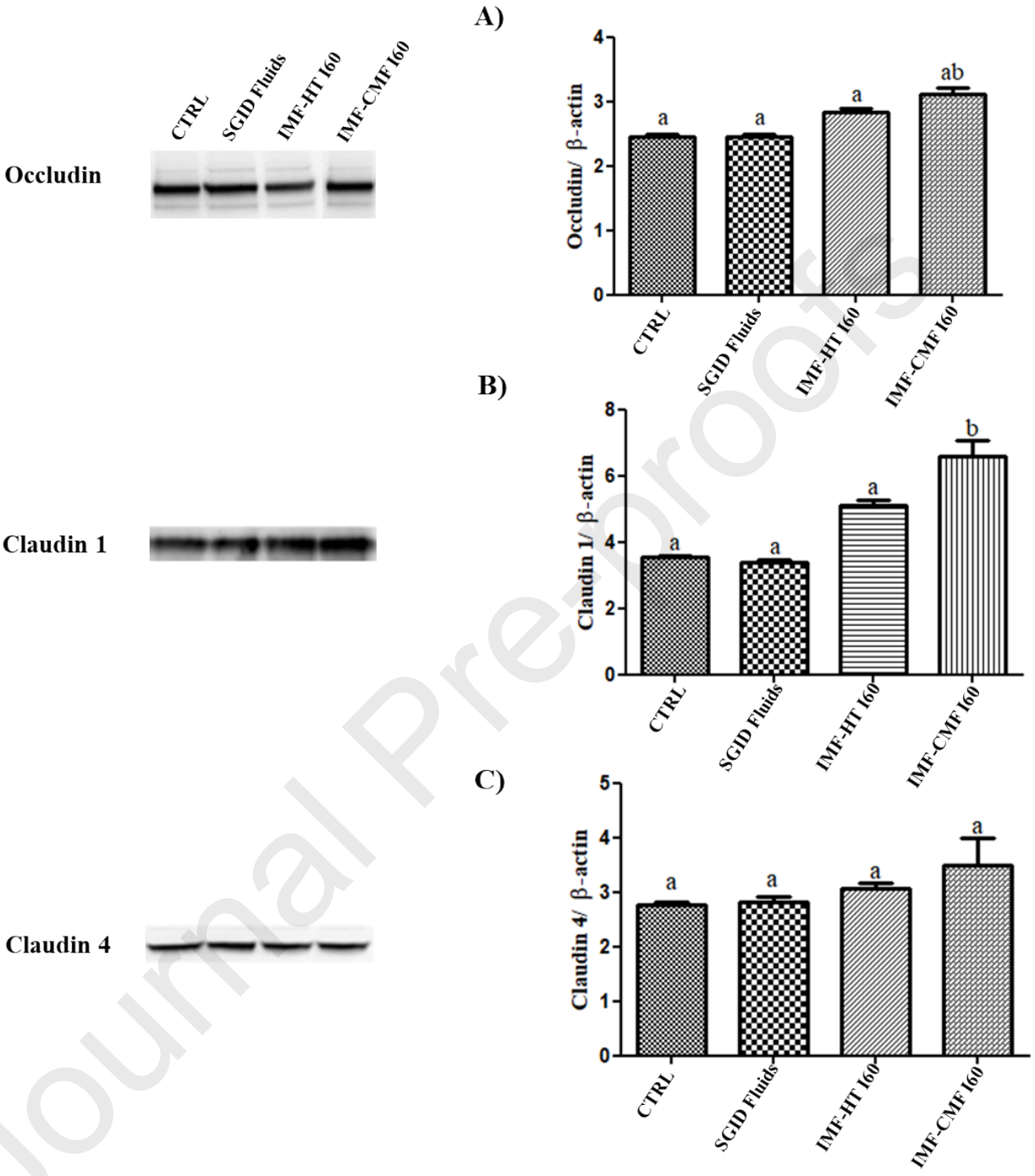

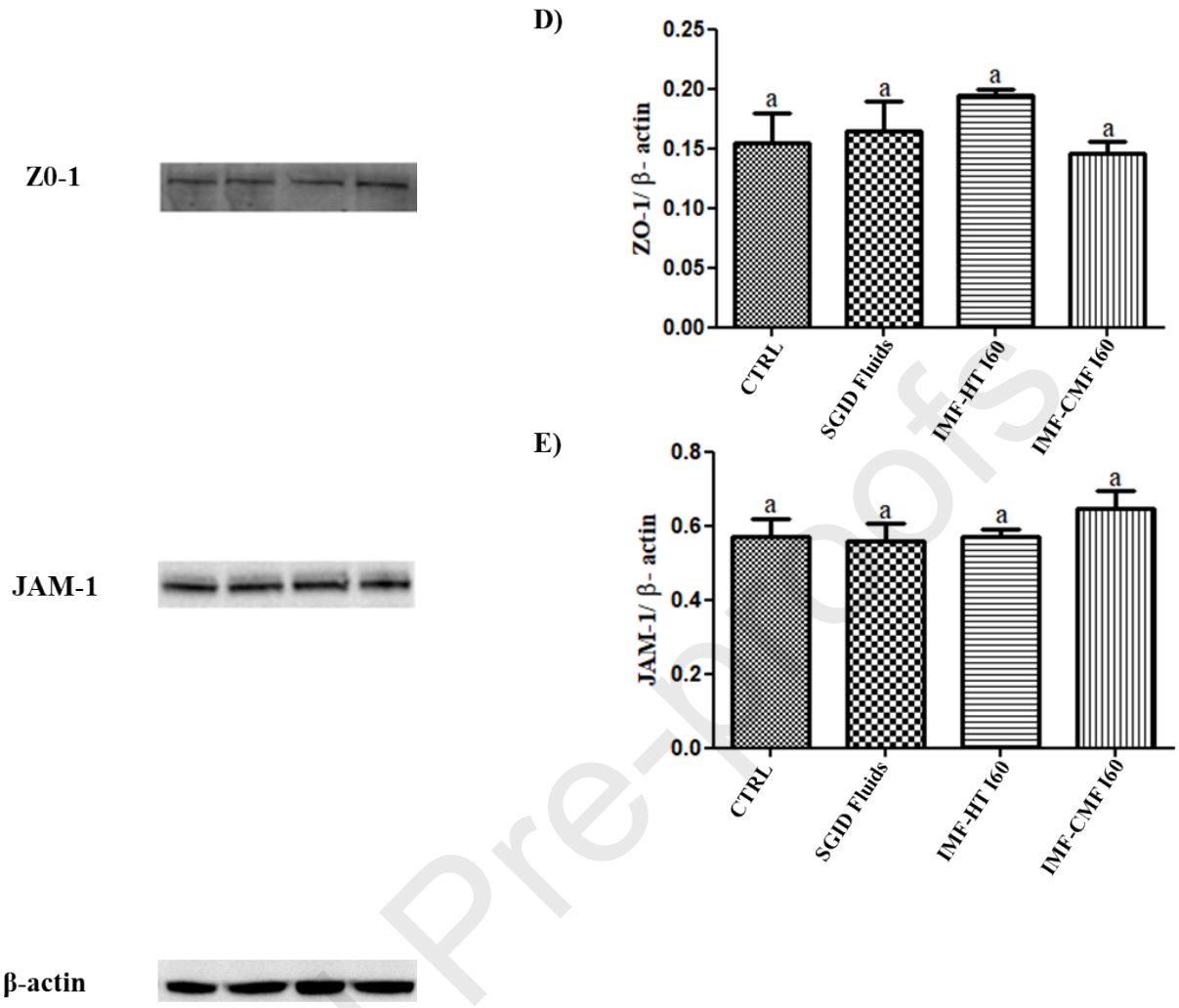

Fig. 3. Western Blot Analysis of Occludin, Caludin 1 and 4, ZO-1 and JAM-1 tight junctions protein in 21 day old differentiated Caco-2 monolayers exposed for 4h to IMF-HT and IMF-CMF digested samples at time point I60 (200 μg/cm^2).

Positive control (CRTL) = Caco2 monolayers exposed to HBSS buffer only. SGID fluids = Caco-2 monolayers exposed to simulated gastrointestinal digestion fluids and enzymes. Panel A: Occludin western blot and densitometer analysis; Panel B: Claudin 1; Panel C: Claudin 4; Panel D: ZO-1; Panel E: JAM-1. Immunoreactive bands were quantified using Immage Lab 6.0. The diagrams show quantification of the intensity of bands, calibrated to the intensity of the β-actin band. All data represent the results of two different experiments (mean±SEM).

Statistical differences were assessed by one-way ANOVA and Bonferroni multiple-comparisons test, with different letters are significantly different ($p < 0.05$), from each other.

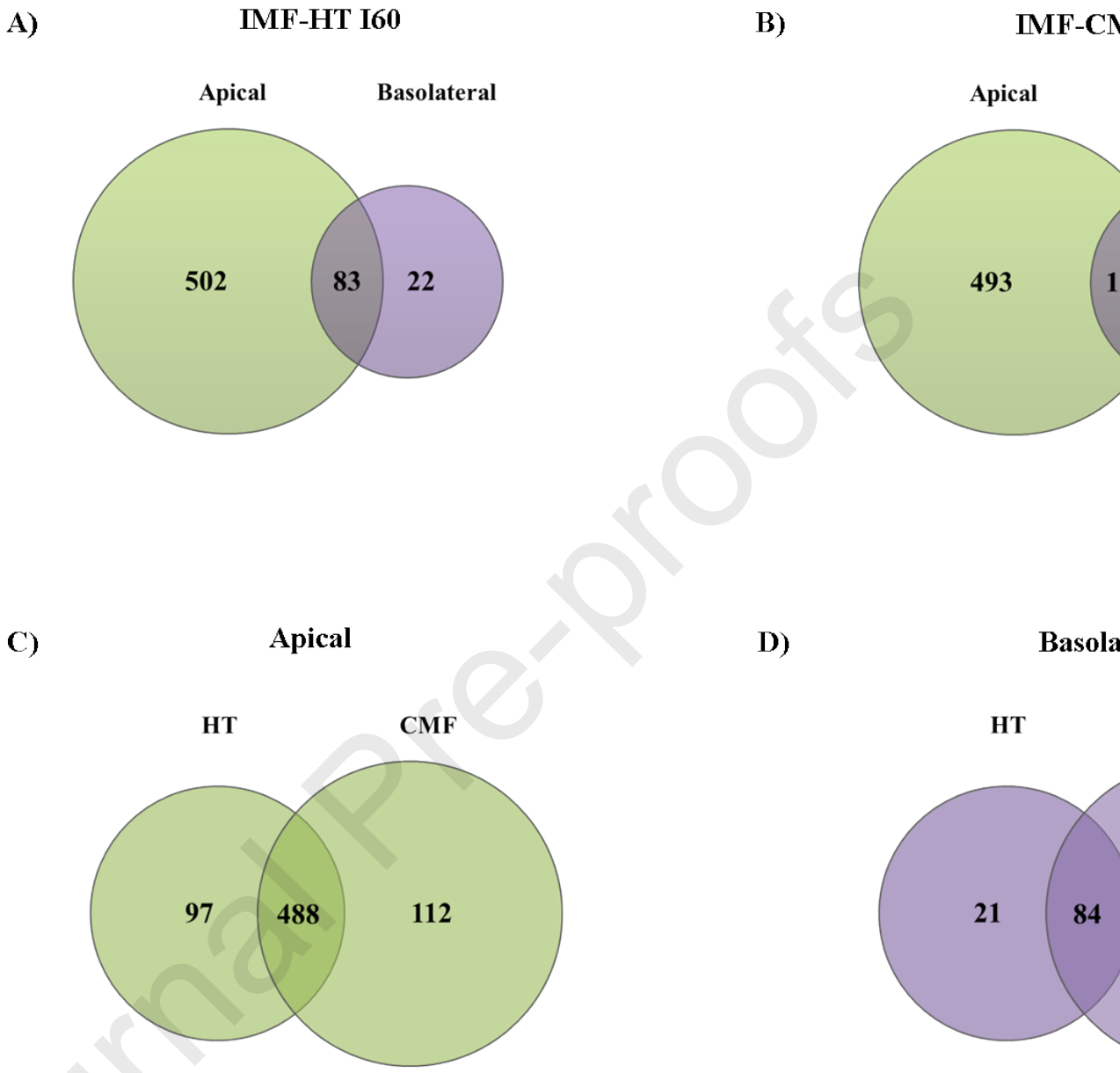

Fig. 4. Venn diagram of individual peptides identified by LC-MS/MS in apical and basolateral compartment of Caco-2 monolayers exposed to the end point of infant gastrointestinal digestion (I60) of infant milk formula (IMF) produced by either high temperature (HT) or cascade membrane filtration (CMF). Differentiated day 21 Caco-2 monolayers were treated for 4 h with either IMF-HT-I60 or IMF-CMF-I60 at 200 µg protein/cm^2. (A) IMF-HT-I60 peptides identified in apical (green), basolateral (purple) and shared peptides (shaded). (B) IMF-CMF-I60 peptides identified in apical (green), basolateral (purple) and shared peptides (shaded). (C)

Caco-2 apical compartment unique peptides from IMF-HT-I60, IMF-CMF-I60 and shared peptides. (D) Caco-2 basolateral compartment unique peptides from IMF-HT-I60, IMF-CMF-I60 and shared peptides.

	IMF-HT			IMF-CMF		
AA, µmol/g of powder	**G0**	**G60**	**I60**	**G0**	**G60**	**I60**
Ala	0.50	0.65	13.24	0.74	0.87	15.80
Arg	0.13	1.67	0.08	0.21	0.15	57.42
Asp	0.43	0.46	5.97	0.34	0.34	5.02
Cys	0.18	0.24	6.58	0.37	0.18	6.43
Cysteic Acid	0.63	0.85	28.09	0.70	1.01	30.16
Gaba	n.d*	n.d	n.d	n.d	n.d	n.d
Glu	2.25	2.46	14.68	2.85	2.76	17.71
Gly	15.40	21.48	25.66	16.12	19.94	27.19
His	0.77	1.09	5.43	0.93	1.11	60.03
Ile	0.07	0.13	13.38	0.15	0.19	13.97
Leu	0.22	0.38	82.06	0.44	0.95	85.94
Lys	0.11	0.17	90.14	0.36	0.28	140.10
Met	0.09	0.09	12.14	0.09	0.16	14.62
Methionine Sulfone	n.d	n.d	n.d	n.d	n.d	n.d
Phe	0.29	0.48	78.86	0.35	0.09	14.13
Pro	0.04	0.17	n.d	0.07	0.12	n.d
Ser	0.22	0.24	6.88	0.33	0.27	7.55
Thr	0.19	0.21	10.62	0.19	0.15	11.00
Trp**	n.d	n.d	3.81	n.d	n.d	4.10
Tyr	0.06	0.09	63.13	0.11	0.12	66.09
Val	0.13	0.23	26.67	0.57	0.42	26.44
Total	21.81	31.09	511.75	24.92	29.15	603.63

Table 1. Free AA released from 1 g of powder of IMF-HT and IMF-CMF gastrointestinal digested at time points; G0=gastric phase time zero, G60=gastric phase at 60mins, I60=intestinal phase at 60mins. Free AA were quantified using a Jeol JLC-500/V amino acid analyser, with one exception: tryptophan.

*n.d= not detected

**= Trp concentration was obtained by GC-MS analysis.

AA (nM)	Compartment	I60	
		IMF-HT	IMF-CMF
Ala			
	Apical	68.6	77.0
	Basolateral	26.4	27.1
Arg			
	Apical	15.9	16.4
	Basolateral	16.5	19.2
Asp			
	Apical	n.d	n.d
	Basolateral	n.d	n.d
Cys			
	Apical	10.6	10.5
	Basolateral	18.3	13.4
Cysteic Acid			
	Apical	10.9	11.1
	Basolateral	12.0	17.6
Gaba			
	Apical	n.d	n.d
	Basolateral	n.d	n.d
Glu			
	Apical	n.d	n.d
	Basolateral	n.d	n.d
Gly			
	Apical	31.2	33.8
	Basolateral	16.4	10.3
His			
	Apical	20.7	20.9
	Basolateral	22.6	24.6
Ile			
	Apical	29.4	34.5
	Basolateral	6.3	7.0
Leu			
	Apical	65.6	76.7
	Basolateral	10.0	18.9
Lys			
	Apical	51.0	60.1
	Basolateral	8.6	9.9
Met			
	Apical	n.d	n.d
	Basolateral	n.d	n.d
Phe			
	Apical	24.7	27.5
	Basolateral	9.1	6.4
Pro			
	Apical	27.7	30.0
	Basolateral	n.d	25.5
Ser			
	Apical	27.5	29.6
	Basolateral	4.2	6.4

Thr			
	Apical	38.5	21.5
	Basolateral	7.8	10.9
Tyr			
	Apical	18.8	21.9
	Basolateral	4.6	4.7
Val			
	Apical	42.8	47.4
	Basolateral	19.9	19.0
Total			
	Apical	484.8	519.7
	Basolateral	187.7	220.9

Table 2. Free amino acids (nM) in apical and basolateral compartments of Caco-2 monolayer after 4 hours incubation with IMF-UHT and IMF-CMF samples at time points I60 (200 μg protein/cm^2).

n.d*=not detected

Credit Author Statement

LG, AB and MC secured funding, conceived and designed the study. SB, YC, GM and GP performed the experiments. SB, LG, GM and GP analysed and interpreted the data. SB and LG drafted the manuscript. All authors revised the manuscript.

.

Highlights

- IMF-CMF slows the rate of protein hydrolysis in the *in vitro* infant stomach
- IMF processing can alter bioaccessibility and bioavailability of peptides
- HT and CMF processing of IMF alters intestinal barrier integrity differently